

Torque and longitudinal force exerted by eigenmodes on circular waveguides

Amit Mizrahi*

Department of Electrical and Computer Engineering, University of California-San Diego, 9500 Gilman Drive, La Jolla, California 92093-0407, USA

Moshe Horowitz and Levi Schächter

Department of Electrical Engineering, Technion-Israel Institute of Technology, Haifa 32000, Israel
(Received 6 February 2008; revised manuscript received 2 July 2008; published 5 August 2008)

It is demonstrated that rotating waveguide eigenmodes may exert a longitudinal force, positive or negative, as well as a torque on the guiding structure itself or part of it. Configurations that are considered include a lossy dielectric cylinder bounded by a hollow waveguide, and a lossy dielectric fiber. Both propagating and evanescent eigenmodes are considered. The analysis is based on a general formulation of the linear and angular momentum currents flowing in the waveguide. The results of this study suggest a novel type of light-driven machine.

DOI: [10.1103/PhysRevA.78.023802](https://doi.org/10.1103/PhysRevA.78.023802)

PACS number(s): 42.25.Bs, 78.70.-g, 03.50.De, 42.50.Tx

I. INTRODUCTION

In an early experiment by Beth [1], it was demonstrated that circularly polarized light can rotate a birefringent plate. Since the introduction of laser-induced optical forces [2], vast research has been devoted to the trapping and manipulation of neutral particles [3]. In particular, use of the rotation of objects due to the torque exerted by laser beams has been suggested for rotating machines. Gaussian laser beams with elliptical polarization were used to trap and rotate birefringent particles [4], and the rotating particles were harnessed to drive a micromotor [5]. Another mechanism for the rotation of particles is through absorption, either by circularly polarized light [6,7], where the torque is proportional to the absorption cross section, or by rotating light with a helical phase front [7,8]. The latter has an angular dependence of the fields of the form $\exp(-jm\phi)$, the integer m being the azimuthal index.

Recently, there has been an interest in optical forces exerted by guided waves on the guiding structure [9–13]. Waveguide eigenmodes are appealing for use in light-driven machines as they have the advantage of being confined, and thus may be integrated into complex systems. In the aforementioned studies, the transverse forces exerted by waves propagating in the longitudinal direction were investigated. It is obvious, however, that guided light carries momentum in the longitudinal direction as well [14], and in this regard it was suggested to use a backscattering resonance to accelerate a dielectric particle in a metallic transmission line [15]. Moreover, in addition to linear momentum, rotating eigenmodes carry angular momentum, the density of which was calculated for a dielectric fiber [16].

In this study, we demonstrate that rotating eigenmodes may exert a pushing or pulling longitudinal force, as well as a torque on the guiding structure itself or part of it. We begin in Sec. II by rigorously analyzing the fundamental configuration of a dielectric cylinder bounded by a perfectly electric

conducting (PEC) waveguide. Having gained insight into the force and torque as resulting from linear and angular *momentum currents*, we proceed in Sec. III to a general formulation of the two currents in waveguides, based on the vacuum Maxwell stress tensor. Finally, we consider in Sec. IV examples of longitudinally invariant waveguides, namely, a PEC waveguide filled with dielectric and a dielectric rod waveguide.

II. DIELECTRIC CYLINDER BOUNDED BY A HOLLOW WAVEGUIDE

In this section we analyze the longitudinal force and torque exerted by an eigenmode on a dielectric cylinder bounded inside a hollow cylindrical PEC waveguide, as illustrated in Fig. 1. We assume that the eigenmode is incident from the left on the dielectric cylinder of length L and radius a . First, we examine the TM case, where the longitudinal electric field of time dependence $\exp(j\omega t)$ in cylindrical coordinates in each one of the regions $\nu=1,2,3$ is given by

$$E_{z,\nu} = J_m(k_{\perp}r)e^{-jm\phi}(A_{\nu}e^{-\gamma_{\nu}z} + B_{\nu}e^{\gamma_{\nu}z}); \quad (1)$$

$J_m(\cdot)$ is the Bessel function of the first kind with zeros $p_{s,m}$, $k_{\perp} = p_{s,m}/a$, $\gamma_{\nu}^2 = k_{\perp}^2 - \epsilon_{r,\nu}\omega^2/c^2$, the permittivities are $\epsilon_{r,1} = \epsilon_{r,3} = 1$, $\epsilon_{r,2} = \epsilon_r' - j\epsilon_r''$, and $B_3 \equiv 0$. In the hollow region, $\gamma_{1,3} = j\beta$ where β is real if the mode is propagating, and $\gamma_{1,3}$ is real for an evanescent mode, i.e., if the mode is below cutoff. For $m \neq 0$, all field components are nonzero with the exception of H_z , and they can be derived from E_z [17].

Since E_z , E_{ϕ} , and H_r vanish at $r=a$, the PEC cylinder experiences no longitudinal force or torque, as the Lorentz force on the surface charges and surface currents on the conductor equals zero. For the calculation of both the longitudinal force and the torque on the dielectric cylinder, we use the Maxwell stress tensor [18], and in the high-frequency time-harmonic regime it is the time-averaged quantities that are of interest. Thus, the time average of the vacuum Maxwell stress tensor is given by

*amitmiz@ece.ucsd.edu

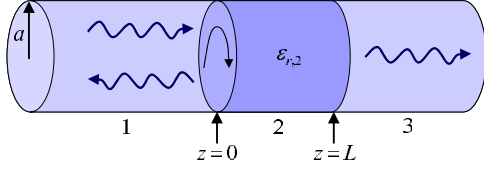


FIG. 1. (Color online). A dielectric cylinder bounded by a hollow PEC waveguide.

$$\langle T_{\alpha\xi} \rangle = \frac{1}{2} \text{Re}(\varepsilon_0 E_\alpha E_\xi^* + \mu_0 H_\alpha H_\xi^*) - \frac{1}{4}(\varepsilon_0 \vec{E} \cdot \vec{E}^* + \mu_0 \vec{H} \cdot \vec{H}^*) \delta_{\alpha\xi}, \quad (2)$$

where $\alpha, \xi = x, y, \text{ or } z$, and $\langle \cdot \rangle$ denotes the time average.

A. Longitudinal force

Defining the vectors $\vec{T}_\alpha \triangleq T_{\alpha x} \vec{1}_x + T_{\alpha y} \vec{1}_y + T_{\alpha z} \vec{1}_z$, where $\vec{1}_\alpha$ is a unit vector in the α direction, the time-averaged longitudinal force reads

$$\langle F_z \rangle = \oiint \langle \vec{T}_z \rangle \cdot d\vec{A}. \quad (3)$$

Taking a surface of integration that encloses the dielectric just outside its boundary, it can be shown that only the $z=0^-$ and the $z=L^+$ planes have nonzero contributions, and we denote the two terms by M_0 and M_L respectively, so that $\langle F_z \rangle \equiv M_0 + M_L$. Beginning with M_L , its explicit integral reads

$$M_L = \iint_{z=L^+} dA \langle T_{zz} \rangle. \quad (4)$$

According to Eq. (3), M_L represents the negative of the *linear momentum current* (momentum per unit time) associated with the outgoing wave. For an incident propagating mode ($\gamma = j\beta$), M_L results from one propagating mode in region 3 ($z > L$), and is given by

$$M_L = -(\beta c/k_0)(P_{\text{tra}}/c^2), \quad (5)$$

where $k_0 \triangleq \omega/c$, and P_{tra} is the transmitted power carried by the mode in region 3. In the $z=0^-$ plane, M_0 consists of self-terms of each of the incident and reflected waves and their cross terms. For the propagating incident mode case, the integral of the cross terms can be shown to vanish, so that the expression for M_0 reads

$$M_0 = \frac{\beta}{k_0} \frac{(P_{\text{inc}} + P_{\text{ref}})}{c}, \quad (6)$$

where P_{inc} and P_{ref} are the powers carried by the incident and reflected waves, respectively. The total longitudinal force therefore reads

$$\langle F_z \rangle = \frac{P_{\text{inc}}}{c^2} v_{\text{gr}} (1 + \mathcal{R} - \mathcal{T}), \quad (7)$$

where $v_{\text{gr}} = \beta c/k_0$ is the group and energy velocity, and \mathcal{R} and \mathcal{T} are the power reflection and transmission coefficients,

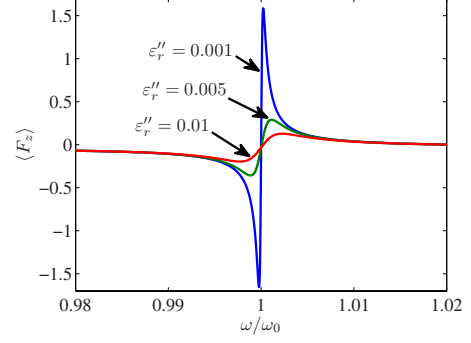


FIG. 2. (Color online) Longitudinal force normalized by $\varepsilon_0 |A_1|^2 \lambda_0^2$ in the vicinity of a resonance in case of an incident evanescent TM mode with $m=1$, for three different values of ε_r'' , and $\varepsilon_r' = 2.1$. The dielectric cylinder has an aspect ratio of $L/a=2$.

respectively. This result is valid for both TE and TM modes, and it indicates that the total force is the sum, with the appropriate sign, of the linear momentum currents of the incident, reflected, and transmitted waves.

When the incident wave is evanescent ($\gamma_{1,3}$ are real), then $M_L=0$, and only the cross products in M_0 give a nonzero integral. The resulting expression for the TM case is

$$\langle F_z \rangle = -\varepsilon_0 |A_1|^2 \pi a^2 \frac{\gamma_1^2}{k_\perp^2} [J'_m(p_{s,m})]^2 \text{Re}(\rho_1), \quad (8)$$

where $\rho_1 \triangleq B_1/A_1$ is the amplitude reflection coefficient, so that $\mathcal{R} = |\rho_1|^2$, and $J'_m(\cdot)$ is the derivative of the Bessel function of the first kind. For a lossless dielectric cylinder, ρ_1 is purely real, and there are resonance frequencies for which it tends to infinity, and around which it changes sign. When losses are introduced, $\text{Re}(\rho_1)$ may change sign as well, as it goes through zero at the resonance frequency. This is demonstrated in Fig. 2 for three different values of ε_r'' , and $\varepsilon_r' = 2.1$. The aspect ratio of the dielectric cylinder is taken to be $L/a=2$, and its lowest resonance frequency for the $m=1$ TM mode is denoted by ω_0 , with a corresponding wavelength $\lambda_0 \approx 2.24a$. The time-averaged longitudinal force $\langle F_z \rangle$ normalized by $\varepsilon_0 |A_1|^2 \lambda_0^2$ is plotted and seen to change sign at the resonance. For higher values of ε_r'' the peak of $\langle F_z \rangle$ is lower. The longitudinal force may, therefore, be positive or negative, meaning that the dielectric cylinder can be pushed by or attracted toward the incoming evanescent wave, depending on the sign of $\text{Re}(\rho_1)$. A similar expression for $\langle F_z \rangle$ may be obtained for the TE case.

B. Torque

Next, the torque on the cylinder is evaluated. The integral of the time-averaged torque [18,19] on the dielectric cylinder with respect to the z axis coinciding with the cylinder axis is simplified to read

$$\langle \tau_z \rangle = \oiint (x \langle \vec{T}_y \rangle - y \langle \vec{T}_x \rangle) \cdot d\vec{A}. \quad (9)$$

It can be shown that the $r=a$ surface does not contribute to this integral, similarly to the calculation of the longitudinal

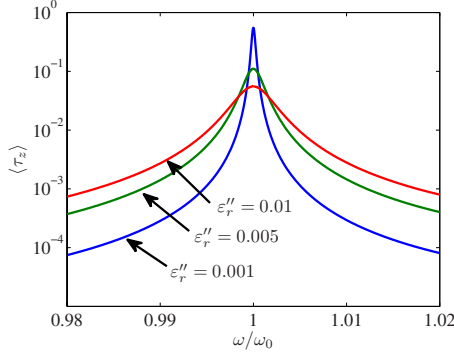


FIG. 3. (Color online) Torque normalized by $\epsilon_0|A_1|^2\lambda_0^3$ in the vicinity of a resonance in case of an incident evanescent TM mode with $m=1$, for three different values of ϵ_r'' , and $\epsilon_r'=2.1$. The dielectric cylinder has an aspect ratio of $L/a=2$.

force. We define N_0 to be the integral on the $z=0^-$ plane and N_L corresponds to the $z=L^+$ plane, so that $\langle \tau_z \rangle = N_0 + N_L$. Transforming the integral to cylindrical coordinates, the expression for N_L explicitly reads

$$N_L = \iint_{z=L^+} dA \frac{1}{2} \epsilon_0 \operatorname{Re}(r E_\phi E_z^*), \quad (10)$$

which represents the negative of the *angular momentum current* of the outgoing wave. For the case of a propagating incident wave, carrying out the above integration gives the result

$$N_L = -\frac{m}{\omega} P_{\text{tra}}. \quad (11)$$

For N_0 , in the case of a propagating incident wave, only the self-terms have a nonzero integral, and consequently it is given by

$$N_0 = \frac{m}{\omega} (P_{\text{inc}} - P_{\text{ref}}). \quad (12)$$

Summing up N_0 and N_L , the total torque reads

$$\langle \tau_z \rangle = \frac{m}{\omega} P_{\text{inc}} (1 - \mathcal{R} - \mathcal{T}), \quad (13)$$

where the negative sign preceding \mathcal{R} , rather than positive as in Eq. (7) for $\langle F_z \rangle$, indicates that *absorption* rather than *reflection* increases the torque. The time-averaged torque may thus be rewritten as

$$\langle \tau_z \rangle = \frac{m}{\omega} P_{\text{abs}}, \quad (14)$$

where P_{abs} is the absorbed power in the dielectric cylinder. A similar expression was obtained for the scattering of a Laguerre-Gaussian beam from a particle [8,20].

For the evanescent case, $N_L=0$, and the nonzero contribution to N_0 comes from the cross terms. The result is that, although Eq. (13) does not hold, Eq. (14) holds for the evanescent case as well, i.e., the torque is proportional to the dissipated power. Figure 3 shows the torque normalized by $\epsilon_0|A_1|^2\lambda_0^3$ in the vicinity of the lowest resonance for the m

$=1$ TM mode, for three different values of ϵ_r'' , and $\epsilon_r'=2.1$. The torque is seen to peak at the resonance frequency. Close to the resonance, the absorption, and with it the torque, decreases with increasing ϵ_r'' , while for frequencies farther away the situation is reversed.

Explicitly for the evanescent case, Eq. (14) may be expressed as

$$\langle \tau_z \rangle = -\epsilon_0|A_1|^2\pi a^2 m \frac{\gamma_1}{k_\perp^2} [J'_m(p_{s,m})]^2 \operatorname{Im}(\rho_1). \quad (15)$$

The imaginary part of ρ_1 is associated with the power flowing into the cylinder, which is facilitated by the existence of both an incoming and an outgoing evanescent wave. Let us normalize $\langle F_z \rangle$ and $\langle \tau_z \rangle$ by $-\epsilon_0|A_1|^2\pi a^2(\gamma_1^2/k_\perp^2)[J'_m(p_{s,m})]^2$, and denote the normalized quantities by $\langle \bar{F}_z \rangle$ and $\langle \bar{\tau}_z \rangle$, respectively. Equation (15) for $\langle \tau_z \rangle$ and Eq. (8) for $\langle F_z \rangle$ may then be expressed by

$$\rho_1 = \langle \bar{F}_z \rangle + j \frac{\gamma_1}{m} \langle \bar{\tau}_z \rangle. \quad (16)$$

Thus, the reflection coefficient for an evanescent incident mode has a strong relation to both the longitudinal force and the torque.

Equation (13) for the torque exerted by propagating waves and Eq. (14) for both propagating and evanescent waves are valid also for the TE case.

C. Discussion

An alternative approach for an analytic calculation of the force and torque on the dielectric cylinder is to consider the Lorentz force density on the effective polarization charges and currents [19]. This treatment has recently been used for several optical configurations (for example, see Refs. [21,12]). While both approaches, the stress tensor approach and the polarization sources approach, result in the same total quantities, the polarization approach has the advantage of obtaining the force and torque volume and surface distributions as well.

Denoting the polarization density by $\vec{\mathcal{P}}$, the effective charge density is given by $\rho_p = -\vec{\nabla} \cdot \vec{\mathcal{P}}$ and the effective time-averaged current density is given by $\vec{J}_p = j\omega\vec{\mathcal{P}}$. Inside a dielectric body, we have $\vec{\mathcal{P}} = \epsilon_0(\epsilon_r - 1)\vec{E}$, where ϵ_r is the relative permittivity. Consequently, for a homogeneous dielectric body, due to Gauss' law, there is no volume polarization charge density, but only surface charge on the boundaries of the dielectric.

For both TE and TM cases, the polarization surface charge density on the $r=a$ surface has no contribution to the force and torque due to the vanishing of E_z and E_ϕ . For the TM case only, there are surface charge densities at the $z=0$ and $z=L$ planes. The contribution of these surface charges to the longitudinal force is due to the *average* between the values of E_z on both sides of the discontinuity. The contribution from the two surfaces to the torque is due to E_ϕ , and for the case of a lossless dielectric, the torques developed on the two planes are equal in magnitude and opposite in sign. For both

the TE and TM cases there is a polarization volume current density $j\omega\epsilon_0(\epsilon_{r,2}-1)\vec{E}$. This current density is responsible for part of the longitudinal force as well as the torque. For the torque, however, there is a time-averaged contribution only if there are losses. Explicitly, for the TM case, the azimuthal force density inside the dielectric cylinder is given by

$$\langle f_\phi \rangle = m \frac{\epsilon_0 k_0^2 |E_{z,2}|^2}{2 k_\perp^2 r} \epsilon_r'' \quad (17)$$

which vanishes for a symmetric mode ($m=0$) or a lossless dielectric ($\epsilon_r''=0$).

The orders of magnitude of the longitudinal force and the torque per unit power can be estimated using the above results. In the case of a propagating incident mode, the longitudinal force per unit power obtained according to Eq. (7) is

$$\frac{\langle F_z \rangle}{P_{\text{inc}}} = \frac{v_{\text{gr}}}{c} (1 + \mathcal{R} - \mathcal{T}) \times 0.33 \times 10^{-8} \frac{\text{N}}{\text{W}}, \quad (18)$$

so that it is upper bounded by the value for $\mathcal{R}=1$ and $v_{\text{gr}}=c$ which is $0.66 \times 10^{-8} \text{ N/W}$. The torque per unit power [Eq. (13)], assuming, for instance, a wavelength of $1.55 \mu\text{m}$, is given by

$$\frac{\langle \tau_z \rangle}{P_{\text{inc}}} = m(1 - \mathcal{R} - \mathcal{T}) \times 0.25 \times 10^{-13} \frac{\text{N m}}{\text{W}}. \quad (19)$$

For comparison, micrometer-sized bodies were shown to rotate due to a torque of less than 10^{-15} N m [5].

Based on the dependence of the two quantities $\langle F_z \rangle$ and $\langle \tau_z \rangle$ on the various parameters of the problem, the dielectric cylinder may be pushed, pulled, and rotated by the incoming mode, if free to move inside the waveguide. For example, having the dielectric cylinder both pushed and rotated will cause a spiral motion that can be used for a light-driven drill.

III. GENERAL FORMULATION

It is now possible to develop a general formulation for the effect of a rotating eigenmode, TE, TM, or hybrid, on a circular waveguide that may have variations along the z direction. As discussed above, the Lorentz force on the waveguide may be viewed as the result of the interaction between the electromagnetic field and the effective polarization charges and currents. In the framework of representation of dielectric materials by effective polarization sources, we may then consider an *equivalent* problem in which the same charges and currents, ρ_p and \vec{J}_p , representing the dielectric material, are interacting in free space with the electromagnetic eigenmode. Since the fields remain the same in the equivalent problem, the different force and torque densities are unchanged as well. It is therefore clear that the Maxwell stress tensor in *vacuum*, rather than the tensor defined using the dielectric constant of the material [14], ought to be used for the calculation of the force and torque on some segment of the waveguide. Correspondingly, it is the Maxwell stress tensor in vacuum that describes the propagation of both the linear and angular momentum in the waveguide.

Specifically, for the linear momentum, we define similarly to the quantity given in Eq. (4)

$$M = \iint dA \langle T_{zz} \rangle, \quad (20)$$

where the integration is over the waveguide cross section. This is, in fact, the negative of the linear momentum current (being negative for a mode propagating in the positive z direction) flowing in the waveguide. A similar definition was considered in Ref. [14]. Assuming that the mode is confined, i.e., the fields vanish for $r \rightarrow \infty$, the longitudinal force on some segment of the waveguide is given by the difference between the outgoing and incoming values of M according to Eq. (3).

For the angular momentum, Eq. (10) is generalized for a hybrid mode to read

$$N = \iint dA r \frac{1}{2} \text{Re}(\epsilon_0 E_\phi E_z^* + \mu_0 H_\phi H_z^*), \quad (21)$$

which represents the negative of the angular momentum current flowing in the waveguide. According to Eq. (9), the torque on a waveguide segment is given by the difference between the outgoing and incoming values of N . It is evident that for a longitudinal force or a torque to develop in the waveguide, the respective momentum current must exhibit a change along z . Such a change could be, for instance, due to a waveguide discontinuity, as in the configuration of Fig. 1, or absorption.

Discontinuities in the permittivity along the waveguide need to be handled carefully. If the electromagnetic mode has a TM part, i.e., a nonzero E_z , then at the discontinuity a polarization surface charge density is formed, and E_z is discontinuous. The surface charge density is due in part to each one of the materials at the two sides of the interface. Calculation of the force and torque on a waveguide segment up to the discontinuity may be done by postulating an infinitesimal vacuum gap between the two materials [12], and calculating the momentum currents in the gap. Then the force and torque on each one of the waveguide segments may be obtained.

IV. LONGITUDINALLY INVARIANT WAVEGUIDES

One important situation where the above formulation is useful is an absorptive waveguide with no variations along the z direction. We assume that a single eigenmode is propagating along the waveguide, having longitudinal dependence of $\exp(-j\beta z)$, where $\beta = \beta_R - j\beta_I$. As a first example that allows for analytic expressions to be obtained, we consider a PEC cylinder filled with a lossy dielectric material, as illustrated in Fig. 4(a). It was already mentioned that the PEC cylinder itself does not experience any longitudinal force or torque, so it is only the dielectric cylinder inside that is affected. Both the linear momentum current and the flowing power P decay exponentially according to $\exp(-2\beta_I z)$, and therefore their ratio is equal to the ratio between the longitudinal force in some segment and the absorbed power P_{abs} in that segment. For a TM mode this ratio is given by

$$\langle F_z \rangle / P_{\text{abs}} = -M/P = \frac{1}{2c} \frac{|\beta|^2 + k_0^2 |\epsilon_r| - k_\perp^2}{k_0 (\epsilon_r' \beta_R + \epsilon_r'' \beta_I)}, \quad (22)$$

and for the TE mode this ratio reads

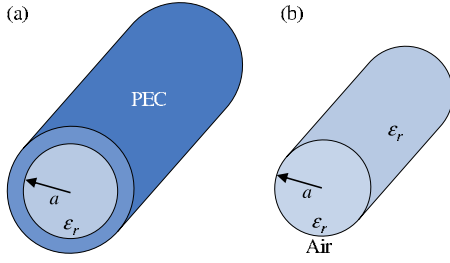


FIG. 4. (Color online) (a) PEC waveguide filled with a dielectric. (b) Dielectric fiber surrounded by air.

$$\langle F_z \rangle / P_{\text{abs}} = -M/P = \frac{1}{2c} \frac{|\beta|^2 + k_0^2 - k_{\perp}^2}{k_0 \beta_R}. \quad (23)$$

For the lossless case and a mode below cutoff, both expressions go to infinity, indicating that a longitudinal force exists although no power is flowing. Remarkably, when the mode is propagating, the momentum current may be opposite to the direction of power flow. For the TE mode, for instance, assuming no losses, the condition for this is $2\beta^2 < k_0^2(\epsilon_r - 1)$, so that, when adding small losses in this situation, the force density is opposite to the power flow.

The ratio between the torque and the absorbed power for the TM case is given by

$$\langle \tau_z \rangle / P_{\text{abs}} = -N/P = \frac{m}{\omega \epsilon_r' + 2\beta_1^2/k_0^2}, \quad (24)$$

having a limiting value for no losses $m/(\omega \epsilon_r)$. For the TE case, this ratio is found to be independent of the permittivity or the geometry, and it reads

$$\langle \tau_z \rangle / P_{\text{abs}} = -N/P = \frac{m}{\omega}. \quad (25)$$

Thus, the mechanical effect of a propagating eigenmode on the waveguide structure is determined by the above four relations [Eqs. (22)–(25)]. The same results were also obtained by calculation of the Lorentz force on the polarization currents.

Based on the concepts presented above, one may contemplate a machine that consists of a lossy waveguide that is rotated and pushed forward by an eigenmode. A realistic example for light frequencies is a lossy dielectric rod waveguide [17], which is a dielectric fiber with air as the cladding, as shown in Fig. 4(b). For this waveguide, the modes are hybrid rather than pure TM or TE. Figure 5 illustrates the force and torque per absorbed power as a function of ϵ_r'' for three cases. The first case considered is the fundamental HE_{11} mode of a dielectric fiber of radius $a=0.5\lambda$, λ being the wavelength, and $\epsilon' = 2.1$. The longitudinal force and the torque per absorbed power are shown in Figs. 5(a) and 5(b), according to Eqs. (20) and (21), respectively. For comparison, the same quantities for the TM_{11} and TE_{11} modes of the PEC waveguide filled with dielectric and having the same radius are depicted using Eqs. (22)–(25). It can be seen that the torque per absorbed power of the HE_{11} dielectric fiber mode is between those of the TM_{11} and TE_{11} PEC modes. Assuming that all the power is absorbed in the waveguide,

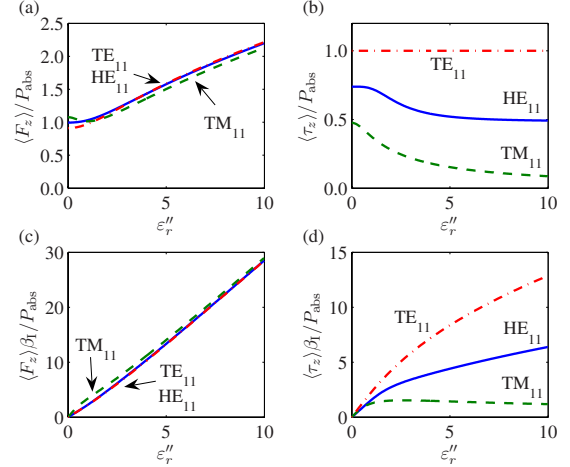


FIG. 5. (Color online). Longitudinal force and torque as a function of the absorption for the TM_{11} mode (dashed) and TE_{11} mode (dash-dotted) of the metallic waveguide filled with dielectric, and HE_{11} mode (solid) of a dielectric fiber. (a) $\langle F_z \rangle / P_{\text{abs}}$ normalized by c^{-1} . (b) $\langle \tau_z \rangle / P_{\text{abs}}$ normalized by ω^{-1} . (c) $\langle F_z \rangle \beta_1 / P_{\text{abs}}$ normalized by $\lambda^{-1} c^{-1}$. (d) $\langle \tau_z \rangle \beta_1 / P_{\text{abs}}$ normalized by $\lambda^{-1} \omega^{-1}$.

the magnitude of the mechanical effect is determined by the force and torque per unit length in which the power is absorbed, which is proportional to β_1^{-1} . The quantities $\langle F_z \rangle \beta_1 / P_{\text{abs}}$ and $\langle \tau_z \rangle \beta_1 / P_{\text{abs}}$ are therefore depicted in Figs. 5(c) and 5(d), respectively, both increasing with ϵ_r'' . Although the torque per absorbed power for the HE_{11} and the TM_{11} mode decreases with increasing ϵ_r'' [Fig. 5(b)], having higher absorption entails that a shorter waveguide with a smaller moment of inertia will absorb the power, resulting in a mechanical effect that increases with ϵ_r'' [Fig. 5(d)].

V. CONCLUSION

In conclusion, the longitudinal force and the torque exerted by a rotating eigenmode on a guiding structure were investigated. The force and the torque were understood in terms of the linear and angular momentum currents, respectively, flowing in a waveguide. This approach is equivalent to the calculation of the Lorentz force on the effective polarization sources.

The fundamental configuration of a dielectric cylinder bounded by a perfect metallic waveguide was analyzed analytically for both propagating and evanescent incident eigenmodes. In addition, longitudinally invariant circular waveguides, including a dielectric fiber, were considered. It was shown that the longitudinal force may be in the opposite direction to the propagation of the eigenmode, whereas the torque, which is proportional to the absorbed power, is in the direction determined by the azimuthal index. However, it follows from the above analysis that for an active medium, i.e., a negative ϵ_r'' , the torque will reverse its sign. The results of this study may be exploited for a novel type of light-driven rotating machines based on guided waves.

ACKNOWLEDGMENTS

This study was supported by the Israel Science Foundation and the Kidron Foundation.

- [1] R. A. Beth, Phys. Rev. **50**, 115 (1936).
- [2] A. Ashkin, Phys. Rev. Lett. **24**, 156 (1970).
- [3] A. Ashkin, IEEE J. Sel. Top. Quantum Electron. **6**, 841 (2000).
- [4] M. E. J. Friese, T. A. Nieminen, N. R. Heckenberg, and H. Rubinsztein-Dunlop, Nature (London) **394**, 348 (1998).
- [5] M. E. J. Friese, H. Rubinsztein-Dunlop, J. Gold, P. Hagberg, and D. Hanstorp, Appl. Phys. Lett. **78**, 547 (2001).
- [6] P. L. Marston and J. H. Crichton, Phys. Rev. A **30**, 2508 (1984).
- [7] N. B. Simpson, K. Dholakia, L. Allen, and M. J. Padgett, Opt. Lett. **22**, 52 (1997).
- [8] H. He, M. E. J. Friese, N. R. Heckenberg, and H. Rubinsztein-Dunlop, Phys. Rev. Lett. **75**, 826 (1995).
- [9] M. L. Povinelli, M. Ibanescu, S. G. Johnson, and J. D. Joannopoulos, Appl. Phys. Lett. **85**, 1466 (2004).
- [10] M. L. Povinelli, M. Lončar, M. Ibanescu, E. J. Smythe, S. G. Johnson, F. Capasso, and J. D. Joannopoulos, Opt. Lett. **30**, 3042 (2005).
- [11] A. Mizrahi and L. Schächter, Opt. Express **13**, 9804 (2005).
- [12] A. Mizrahi and L. Schächter, Phys. Rev. E **74**, 036504 (2006).
- [13] A. Mizrahi and L. Schächter, Opt. Lett. **32**, 692 (2007).
- [14] H. A. Haus and H. Kogelnik, J. Opt. Soc. Am. **66**, 320 (1976).
- [15] R. Gómez-Medina, P. San José, A. García-Martín, M. Lester, M. Nieto-Vesperinas, and J. J. Sáenz, Phys. Rev. Lett. **86**, 4275 (2001).
- [16] F. Le Kien, V. I. Balykin, and K. Hakuta, Phys. Rev. A **73**, 053823 (2006).
- [17] R. E. Collin, *Field Theory of Guided Waves* (McGraw-Hill, New York, 1960).
- [18] J. D. Jackson, *Classical Electrodynamics*, 3rd ed. (Wiley, New York, 1975).
- [19] J. Schwinger, L. L. DeRadd, K. A. Milton, and W.-Y. Tsai, *Classical Electrodynamics* (Perseus Books, Reading, MA, 1998).
- [20] L. Allen, M. W. Beijersbergen, R. J. C. Spreeuw, and J. P. Woerdman, Phys. Rev. A **45**, 8185 (1992).
- [21] M. Mansuripur, Opt. Express **12**, 5375 (2004).